Hindawi
Adsorption Science & Technology
Volume 2022, Article ID 9009214, 20 pages
https://doi.org/10.1155/2022/9009214

Research Article

Adsorption of Crystal Violet Dye from Aqueous Solution using Industrial Pepper Seed Spent: Equilibrium, Thermodynamic, and Kinetic Studies

Razia Sulthana,[1] Syed Noeman Taqui,[2,3] Usman Taqui Syed,[4] T. M. Yunus Khan,[5] Shaik Dawood Abdul Khadar,[6] Imran Mokashi,[7] Kiran Shahapurkar,[8] M. A. Kalam,[9] H. C. Ananda Murthy,[10,11] and Akheel Ahmed Syed[3]

[1]*Department of Studies in Chemistry, University of Mysore, Manasa Gangothri, Mysuru 570006, India*
[2]*Department of Chemistry, School of Technology, Glocal University, Delhi-Yamunotri Marg, SH-57, Mirzapur Pole, Saharanpur District, Uttar Pradesh 247121, India*
[3]*Centre for Advanced Research and Innovation, Glocal University, Delhi-Yamunotri Marg, SH-57, Mirzapur Pole, Saharanpur District, Uttar Pradesh 247121, India*
[4]*LAQV-REQUIMTE, Department of Chemistry, Faculty of Science and Technology, Universidade NOVA de Lisboa, 2829-516 Caparica, Portugal*
[5]*Mechanical Engineering Department, College of Engineering, King Khalid University, Abha 61421, Saudi Arabia*
[6]*Industrial Engineering Department, College of Engineering, King Khalid University, Abha 61421, Saudi Arabia*
[7]*Department of Mechanical Engineering, Bearys Institute of Technology (Affiliated to Visvesvaraya Technological University), Mangalore, Karnataka, India*
[8]*Department of Mechanical Engineering, School of Mechanical, Chemical and Materials Engineering, Adama Science and Technology University, Adama, P O Box 1888, Ethiopia*
[9]*School of Civil and Environmental Engineering, FEIT, University of Technology Sydney, Sydney, NSW 2007, Australia*
[10]*Department of Applied Chemistry, School of Applied Natural Science, Adama Science and Technology University, Adama, P O Box 1888, Ethiopia*
[11]*Department of Prosthodontics, Saveetha Dental College & Hospital, Saveetha Institute of Medical and technical science (SIMAT), Saveetha University, Chennai, 600077 Tamil Nadu, India*

Correspondence should be addressed to H. C. Ananda Murthy; anandkps350@gmail.com

Received 7 May 2022; Revised 15 July 2022; Accepted 24 August 2022; Published 13 September 2022

Academic Editor: Lakshmipathy R

The economic viability of adsorbing crystal violet (CV) using pepper seed spent (PSS) as a biosorbent in an aqueous solution has been studied. A parametrical investigation was conducted considering parameters like initial concentration of dye, time of contact, pH value, and temperature variation. The analysis of experimental data obtained was carried out by evaluating with the isotherms of Freundlich, Sips, Tempkin, Jovanovic, Brouers–Sotolongo, Toth, Vieth–Sladek, Radke–Prausnitz, Langmuir, and Redlich–Peterson. The adsorption kinetics were studied by implementing the Dumwald-Wagner, Weber-Morris, pseudo-first-order, pseudo-second-order, film diffusion, and Avrami models. The experimental value of adsorption capacity ($Q_m = 129.4\,\mathrm{mg\,g^{-1}}$) was observed to be quite close to the Jovanovic isotherm adsorption capacity ($Q_m = 82.24\,\mathrm{mg\,g^{-1}}$) at ($R^2$), coefficient of correlation of 0.945. The data validation was found to conform to that of pseudo-second-order and Avrami kinetic models. The adsorption process was specified as a spontaneous and endothermic process owing to the thermodynamic parametrical values of ΔG^0, ΔH^0, and ΔS^0. The value of ΔH^0 is an indicator of the process's physical nature. The adsorption of CV to the PSS was authenticated from infrared spectroscopy and scanning electron microscopy images. The interactions of the CV-PSS system have been discussed, and the observations noted suggest PSS as a feasible adsorbent to extract CV from an aqueous solution.

1. Introduction

Advanced wastewater treatment methods and technologies are critical for ensuring maximum water quality and removing heavy metals, dyes, and other pollutants from water [1]. Fabrics or surfaces are colored by impregnating using chemical compounds called dyes. Synthetic dyes have been extensively used in the textile, paper making, pharmaceutical, and food packaging industries. The improper methods of processing and dying followed by most of these industries have resulted in the release of tons of dyes in aquatic resources (40,000–50,000 tons). The adverse effects of releasing dyes untreated into water sources have disastrous implications on human health and marine ecology. The dyes are potentially cancer-causing, teratogenic, or mutagenic to the aquatic species. Severe dysfunctions in the human reproduction system, brain, kidney, liver, and nervous system are potential repercussions [1]. Light penetration in water is hampered due to colored dyes, which creates difficulty for the water life processes. Thus, the treatment of industrial wastewater to remove dye traces is essential [2]. The wastage of synthetic dye is about 12% and has been estimated during manufacturing, and 20% of this is released as effluent industrial water waste [3].

The dye content in the industrial wastewater discharge pollutes the water body by causing discoloration, thereby hindering sunlight penetration, resulting in restricting the biological and photochemical processes in water sources [4]. The data reveals the availability of 1 lakh dyes of commercial-grade manufactured at the rate of 7×10^5 tons annually [5]. The annual dye consumption has been estimated to be ten thousand tons worldwide, and nearly one hundred tons of untreated dye is released annually as industrial waste into water sources [6].

In the dyeing of paper, nylon, cotton, leather, silk, wool, and others, crystal violet forms a primary dyeing constituent. CV is a highly graded soluble dye with distinct dyeing properties. A quantity of $1\,mg\,L^{-1}$ less is capable of coloration, which clarifies the requirement of treating wastewater of dye contamination [7]. CV is a triarylmethane class of dye that is carcinogenic and can produce severe irritation in the eyes if accidentally consumed or contacted through the skin [8].

Several processes for removing synthetic dyes from the industrial water discharge have been suggested in the literature. The processes are as follows: Fenton process [9], photocatalysis [10], integrated chemical biodegradation [11], electrochemical method [12], and adsorption [13–17]. The economic viability and operational simplicity adjunct with component revival, recovery, and reuse have credited adsorption as the most feasible dye removal technique from wastewater solutions [18]. Activated carbon as an adsorbent for dye removal requires a considerably high cost and is difficult to regenerate. This necessitates the procurement and development of alternate economic adsorbents [19]. Concerning the environmental and health hazards posed due to contamination of water bodies by industrial dyeing, it is of high importance to treat the effluents before discharging them into water sources [20], and in doing, so the adsorption method of wastewater treatment has been reported to be more efficient [21].

The agricultural wastes such as rice husk [3], waste from ginger [22], soya oil extract [23], peelings of lemon [24], cane sawdust [25], tamarind shells [26], maize [27], powder of seashells [28], and papaya fruit seeds [29] are low-cost adsorbents.

Black pepper (*Piper nigrum*) is a spice related to the *Piperaceae* family originating from southern India but is widely grown in tropical places. Vietnam is the world's highest pepper harvester producing about 34% of the world's *Piper nigrum*, also termed Black Gold. Pepper is a spice 5 mm in diameter, and its black color is ascribed to the piperine chemical. In dried form, it is utilized as a flavoring agent for its peculiar taste and medicinal purposes.

Table 1 lists several adsorbents implemented for CV removal from industrial dye wastewater and their maximum crystal violet uptake (Q_e) values. The adsorbent desired should be mainly available and at a low cost. It should not require prechemical handling and must be available for direct use. It should possess the characteristics of porosity to enhance adsorption.

The parameters identified for efficient handling of effluents generated in large volumes by industries like textile and others can be sufficed through nutraceutical industrial spent (NIS), which are available in plenty. Besides, the NIS has qualities that have not been reported for any other adsorbents. Nutraceuticals are thermally, mechanically, and chemically processed to extract the principal component(s) before being discarded in industry. Thus, the NIS requires no chemical treatment before it is used to remediate CV from waters and industrial effluents. This will add to the advantage of reducing the E-factor [48]. The fibril structure of PSS will trap moisture content, reduce the calorific value, and enhance the emission of toxic gases. Conversely, the same property can be utilized to enhance the sorption of toxic dyes on PSS.

The present research aims to study the adsorption characteristic of PSS, a nutraceutical industrial spent possessing the desired qualities of an excellent biosorbent to remove harmful CV from industrial wastewater at a low cost. Morphological and structural analyses of the adsorbents were conducted. The kinetic study, adsorption isotherms, and thermodynamics related to this adsorption process have been simulated and described comprehensively.

Our research school has demonstrated pioneering efforts to use NIS as filler material for the fabrication of composites [49–52] and as an adsorbent for the bioremediation of toxic dyes [53–64]. Recently, our research school has demonstrated circular economy at the laboratory scale using NIS [65].

The novelty of this work lies in the nutraceutical industrial pepper seed spent which is an environmental-friendly and cost-effective biosorbent to remediate the toxicity of the dye due to the presence of crystal violet in textile industry wastewater. Lastly, the experimental results were complimented with the modeling studies, and the adsorbent regeneration with cost analysis was also investigated.

Table 1: The adsorption capacity of different materials derived from agricultural biomass.

Crystal violet	Qe (mg g^{-1})	References
Coir pith	2.56	[30]
Sepiolite	2.69	[31]
Sugarcane sawdust	3.80	[32]
Neem wood sawdust	3.80	[32]
Calotropis procera leaves	4.14	[33]
Sagun sawdust powder	4.25	[34]
Sugarcane fiber strands	10.44	[35]
Citrullus lanatus rind	10.54	[36]
Jalshakti polymer material	12.90	[37]
Orange fruit peelings	14.30	[38]
Apple wood	19.80	[39]
Bagasse fly ash	26.25	[40]
Carbon jute fiber	27.99	[41]
Powder of coniferous pinus bark	32.78	[42]
Sawdust powder	37.83	[35]
Bran of rice	42.25	[43]
Powder of jackfruit leaf	43.39	[44]
Treated ginger waste	64.90	[45]
Bran of wheat	80.37	[46]
Skin almond waste	85.47	[47]
Male flower activated carbon of coconut tree	85.84	[18]
Pepper seed spent	87.26	This study

2. Materials and Methods

2.1. Adsorbate. Crystal violet (CV), [M.F. = $C_{25}H_{30}ClN_3$, M .W. = 407.988 g/mol, and λ_{max} = 590 nm], was bought from Sigma Aldrich Private Ltd., Mumbai. CV solution was made by using double-distilled water for dissolving a calculated quantity of dye. Figure 1 represents the CV molecular structure.

2.2. Preparation of Adsorbent. The PSS utilized in the present study was generously granted by M/s. Sami Labs, Bengaluru, India. The spent was washed of impurities like dust using distilled water and dried by baking for 24 hours at 60°C in an oven. After drying, the spent is processed to obtain a particle size ≤177 μm using a sieve of 80 mesh size. The spent particles are stored in plastic bottles without treating chemically or physically for future use.

2.3. Surface Characterization. The morphology of PSS surface was examined using scanning electronic microscope (SEM) (LEO 435 VP model, Japan). FTIR spectrometer (Inter-spec 2020, Spectro Lab, UK) was utilized to identify the adsorbent feature of the PSS. The infrared images before CV adsorption and after adsorption to PSS in the control samples were recorded. The surface charge was determined by pH_z (point of zero charge) value.

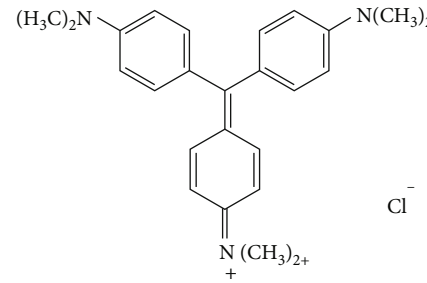

Figure 1: Crystal violet molecular structure.

2.4. Experimental Study of Adsorption. The experimental study was conducted employing the technique of batch adsorption. A known quantity of PSS (50 mg) was added to a dye concentration range (25-200 mg L^{-1}) in an Erlenmeyer flask of 250 ml. The solution is stirred at a constant rpm of 170 for 180 minutes under isothermal conditions to achieve a uniform solution [66]. At equilibrium and $t = 0$, the dye concentration was analyzed using distilled double beam UV spectrophotometer (systronics model 117, USA) at 590 nm. The quantity of adsorbed CV, q_e (mg g^{-1}), was calculated using

$$q_e = (C_0 - C_e) * \frac{V}{W}, \quad (1)$$

where C_0 and C_e are initial and equilibrium CV concentrations in (mg L^{-1}), respectively, V is the volume of the solution (l), and W is the weight of the adsorbent (g).

The study of batch kinetics was conducted on similar lines in measuring CV concentrations in the aqueous solution, but the measurements were done for preset intervals of time. The quantity of adsorbed CV adsorbed at any time interval, q_t (mg g^{-1}), was determined using

$$q_t = (C_0 - C_t) * \frac{V}{W}, \quad (2)$$

where C_t is CV concentration in the liquid phase at any time (mg L^{-1}). Initial dye concentrations were established between 50 and 200 mg L^{-1} in increments of 50 mg L^{-1} during a 60-minute adsorption duration (at 5-minute intervals), and the results were analysed.

To investigate the pH effects on dye adsorption, stirring of 50 mg PSS and 50 ml dye solution at 200 mg L^{-1} concentration in an isothermal environment was carried out. For a pH range of 2-12, this experiment was repeated at a constant agitation of 170 rpm for a time period of 180 min. The dye concentration measurement was done at 590 nm using a UV-vis spectrophotometer. The pH meter was used to determine the pH level of the solution, and any adjustments were made by diluting with HCl and NaOH. The quantity of dye removed was calculated using the equation

$$\text{Dye removal\%} = \frac{(C_0 - C_e)}{C_o} \times 100. \quad (3)$$

Table 2: Details of two parameters and three-parameter isotherm models.

Two parameter isotherms		Three parameter isotherms	
Langmuir	$q_e = Q_m K_a C_e / 1 + K_a C_e \; R_L = 1/1 + K_a C_0$	Sips	$q_e = \dfrac{Q_m (K_s C_s) m_s}{(1 + K_s C_s) m_s}$
Freundlich	$q_e = K_F C_e^{\,1/n_F}$	Toth	$q_e = Q_m C_e (b_{T0} + C_e n_{T0}) - 1/_{nT0}$
Jovanovic	$q_e = Q_m C_e \left(1 - e^{(K_J C_e)}\right)$	Radke–Prausnitz	$q_e = \dfrac{K_{\mathrm{RP}} Q_m C_e}{(1 + K_{\mathrm{RP}} C_e) m_{\mathrm{RP}}}$
Tempkin	$q_e = \dfrac{\mathrm{RT}}{b_T} \ln (k_T C_e)$	Vieth–Sladek	$q_e = K_{\mathrm{VS}} + \dfrac{Q_m \beta_{\mathrm{VS}} C_e}{1 + \beta_{\mathrm{VS}} C_e}$
Harkins Jura	$q_e = \left[\dfrac{A_{\mathrm{HJ}}}{B_{\mathrm{HJ}} - \log C_e}\right] 1/_2$	Redlich–Peterson	$q_e = \dfrac{A_{\mathrm{RP}} C_e}{1 + K_{\mathrm{RP}} C_e^g}$

Where Q_m is the maximum adsorption capacity; K_a is the Langmuir constant; R_L is the separation factor; K_F and n_F are the Freundlich constants; K_J is the Jovanovic constant; b_T and k_T are the Tempkin constants; R is the universal gas constant; T is the absolute solution temperature in Kelvin; A_{HJ} and B_{HJ} are the Harkins-Jura constants; A_{RP}, B_{RP}, and g are the Redlich–Peterson constants; $b_{T\mathrm{o}}$ and $n_{T\mathrm{o}}$ are the Toth constants; K_{RP} and m_{RP} are the Radke–Prausnitz constants; K_S and m_S are the Sips constants; and K_{VS} and β_{VS} are the Vieth–Sladek constants.

The experiments were done in triplicates, and the results obtained are referenced as the average values of the parameters.

2.5. Modeling Parameter Study

2.5.1. Adsorption Isotherms. The adsorbate and adsorbent interaction is specified by the adsorption study relative to isotherms. The parameters of such a study provide data regarding the interaction methodology, adsorbent affinity, and surface properties. Langmuir and Freundlich's adsorption models for the surface property study provide prudent equations for single solute samples. The contemporary models to these models are Tempkin, Harkins-Jura, SIPS, Redlich-Peterson, Vieth-Sladek, Radke-Prausnitz, and Toth that provide adsorption information at ambient temperature.

The influencing parameters such as Q_m, R^2, and chi-squared test (χ^2) govern the CV_PSS theoretical model development. Table 2 lists the experimental information such as mathematical equations, isotherms, and influencing parameters. This data defines the developed theoretical model.

2.5.2. Kinetics of Adsorption. The adsorption information obtained from the experimental study was analyzed by implementing pseudo-first- and second-order equations and Avrami kinetics and curve-fitting by the least square method. The concerned equations of kinetic models are stated in Table 3. Diffusion models such as the Dumwald-Wagner diffusion model, film diffusion model, and Weber-Morris diffusion models were incorporated to study the diffusion effect. The adsorption controlling mechanism determination concerning the kinetic models integrated with the study is presented in Table 3.

2.5.3. Thermodynamic Parameters. A process practicability and mechanism are explained by the process energy and its entropy. In the current work, the thermodynamic parameters comprising of change in enthalpy (ΔH^0), change in entropy (ΔS^0), and free energy (ΔG^0) were approximated by implementing the rate law conversely to the data obtained from equations in tabulating the adsorption process enthalpy.

Table 3: Nonlinear modes of kinetic models.

Pseudo-first order	$q_t = q_e \left(1 - e^{-k_1 t}\right) \; h_0 = k_1 q_e$
Pseudo-second order	$q_t = q_e^2 k_2 t / 1 + q_e k_2 t \; h_0 = k_2 q_e{}^2$
Avrami	$q_t = qe\{1 - \exp\,[-K_{\mathrm{AV}} t)]n_{\mathrm{AV}}\}$
Film diffusion model	$\ln \left(1 - \dfrac{q_t}{q_e}\right) = -R \;\; ^{\mid} t$
Weber- Morris model	$q_t = k_{\mathrm{int}} t^{1/2}$
Dumwald-Wagner diffusion model	$\log \left(1 - F^2\right) = -\dfrac{K}{2.303} t \; F = \dfrac{q_t}{q_e}$

Where k_1 is the rate constant for the pseudo-first-order adsorption; k_2 is the rate constant for the pseudo-second-order adsorption; h_0 is the initial adsorption rate; k_{AV} and n_{AV} are the Avrami constants; R is the liquid film diffusion constant; k_{int} is the diffusion rate constant; and K is the rate constant of adsorption.

3. Analysis of Experimental Outcomes

3.1. Characteristic Study of Spent Surface

3.1.1. Scanning Electron Microscopy (SEM). PSS surface structure was studied employing scanning electron microscopy. The scanning was carried out for pre- and post-CV adsorption. Figure 2(a) is an SEM image of the PSS surface before adsorption, indicating a fibrous channeled and porous structure, potentially improving dye adsorption. Figure 2(b) pictures the pores and gaps noticed in the PSS structure occupied by the dye due to adsorption.

3.1.2. FTIR Spectroscopy. Figure 3 represents a broad band range relative to the influence of different parameters [67]. The 3291.44/cm band is concerned with the hydroxyl groups relevant to the adsorbed aqua cellulose. 2920.26/cm band is ascribed to vibrational stretching of –CH bond pertinent to alkyl and alkane groups. C=C olefin stretching is analyzed

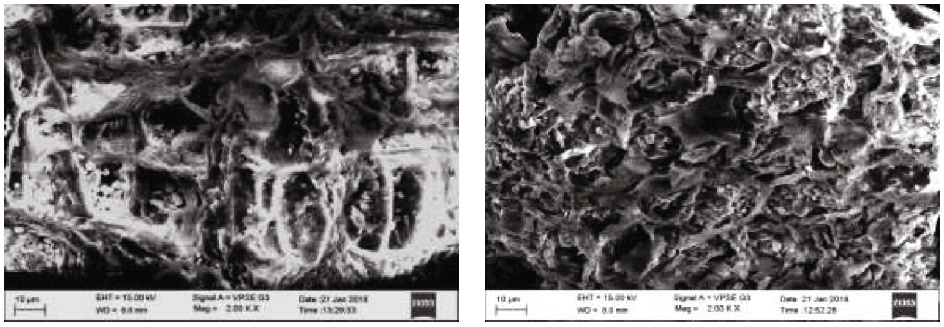

(a) (b)

Figure 2: (a) PSS SEM image before CV adsorption and (b) PSS SEM image after CV adsorption.

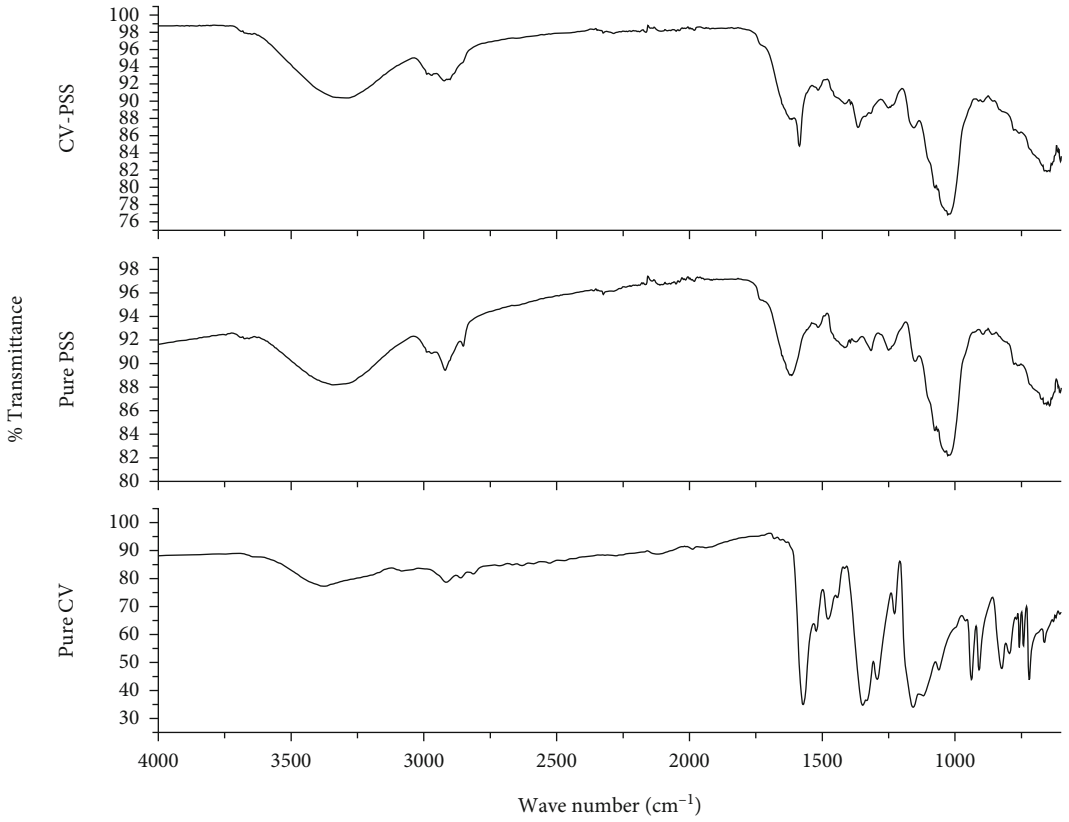

Figure 3: FTIR spectrum of (a) CV, (b) PSS, and (c) CV adsorbed PSS.

as influencing the band 1615.47/cm. Band 1417.32/cm resembles methyl groups. The 1026/cm band is attributed to the cellulose in the adsorbent.

PSS adsorption of CV is ascertained by the 3291.35/cm band of the hydroxyl group. The stretching caused by the –CH bond vibrations results in the shift of band from 2916/cm to 2922.92/cm in carbon and hydrogen-bonded alkane-alkyl groups. On the contrary, there is a decrease in the band 1615.47/cm to 1586.51/cm attributed to the imine group present in CV and stretching of C=C bonds. After adsorption, a reduction in the band from 1417.32/cm to 1365.58/cm is noticed in CH_3 and Caryl-N bond [39]. After adsorption, it was identified and commented that a shift in the peaks was noticed in the reduction of band 1062/cm to 1056.94/cm. It was also suggested that new peaks were formed after adsorption due to the disappearance of some peaks. These variations in the FTIR spectra were attributed to the collaboration of functional groups in the process of adsorption. The range of adsorption bands 1000/cm to 600/cm differed later due to chemical variations.

3.1.3. Point of Zero Charge. The procedure endured to determine the point of zero charge (pH_z) was initiated with the preparation of 0.1 M KCl. The pH of 0.1 M KCl was deliberated within 2-12 utilizing sodium hydroxide and HCl. Next, PSS (0.05 g) is added to 0.1 M KCl (50 ml) in a flask of 250 ml. After an incubation period of 24 hours, the pH value of the solution is measured using a pH meter. Figure 4 is the

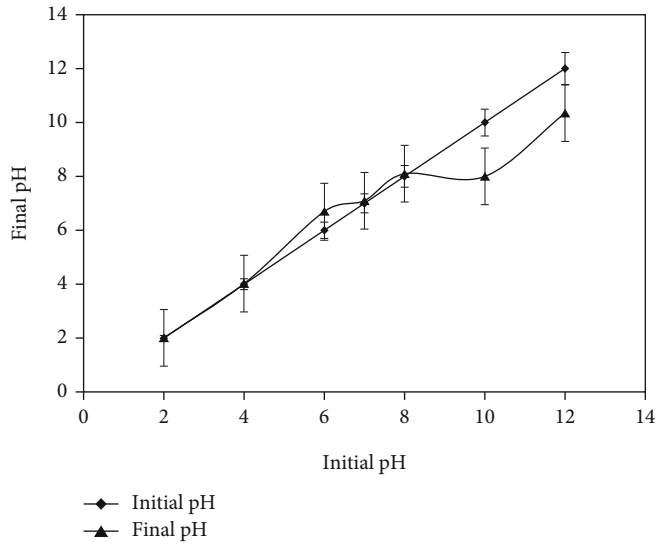

Figure 4: Point of zero charge of PSS.

plot of $pH_{final} - pH_{initial}$. The intersection of the curves is the point of zero charge, recorded as 7.1 for PSS.

3.2. Studies on Batch Adsorption

3.2.1. Effect of Initial Concentration of Dye and Time of Contact. With an initial increase from the 25 to 200 mg L^{-1} concentration of dye, a surge in dye adsorption from 15 to 90 mg g^{-1} indicates a rise in the concentration gradient conducting force. Figure 5 expresses the relation between the adsorption of CV and duration contact. The process of adsorption was witnessed to increase with a great extent of contact duration. It can be observed from Figure 5 that after a contact period of 180 min, the CV separation from the solution was maximum. The other relative observations were rapid adsorption of dye onto the external surface during the beginning period and then a slowdown of the process during the adsorption of dye in the pores. At high concentrations, the process of adsorption was swift and decelerated to a constant at equilibrium time.

3.2.2. Adsorbent Quantity Effect. It is critical to determine the minimum adsorbent amount to maximize adsorption. It was calibrated for an adsorbent dosage range of 0.025-0.2 g. It was noticed that with the initial increase in the quantity of adsorbent, the process was expedited. Still, with the continuous addition of the adsorbent, it impeded due to the PSS surface's capturing by dye molecules [28]. Figure 6 reveals that with the rise in the adsorbent, the amount process of adsorption gets enhanced and later it approaches towards equilibrium with increase in adsorbent dosage.

3.2.3. Effect of Adsorbent Dosage. The amount of adsorbent has a critical influence on the adsorption process. The concentration variation controls the adsorption process capacity at working conditions. Figure 6 is a graphical representation of an increase in the adsorption process with an increase in the concentration of the adsorbent [3]. The maximum experimental equilibrium value q_e decreases from 125 to 40 mg g^{-1}, i.e., from 0.05 to 0.20 g L^{-1} adsorbent dosage of NIPSS.

3.2.4. Temperature Effect. The adsorption process investigation was exhibited at 30°C-50°C. Figure 7 shows the temperature variation effect on the process. The adsorption increased considerably with an increase in the temperature, which categorizes the process as exothermic. The dye molecules acquire high kinetic energy, and their intramolecular diffusion is enhanced with an increase in the solution temperature, thereby improving the adsorption [22]. The interaction between CV and PSS occurs because of molecular dye diffusion with temperature rise [68, 69]. The maximum experimental equilibrium value q_e increases marginally with increase in temperature between 303 K and 323 K as depicted in Figure 7.

3.2.5. pH Influence on the Adsorption. One of the processes controlling factors is the solution pH, which improves the adsorption of dye onto PSS with an increase in it by affecting the surface properties and dye ion variation. A peak rise in the adsorption capacity was observed in the acidic range, probably due to a surplus of H^+ ion interaction with the cations along with the dye. With an increase in the pH of the solution, the density of charge is reduced. Figure 8 depicts the increase in the process of adsorption owing to the repulsion among charged dye ions, and the adsorbent surface lowers [70]. The maximum experimental equilibrium value q_e increases with an increase in pH from 15 to 185 mg g^{-1} and 2 to 12.

3.2.6. Particle Size Effect on Adsorption. Absorbent mesh particle sizes of ≤90, ≥90, ≥120 ≥ 177, ≥355, and ≥550 at a CV concentration of 200 mg L^{-1} were investigated for their influence on the adsorption process. Figure 9 describes that there is a drop in the adsorption process with an increase in the particle size. This can be reasoned as due to smaller size of particles increases the surface area contrary to

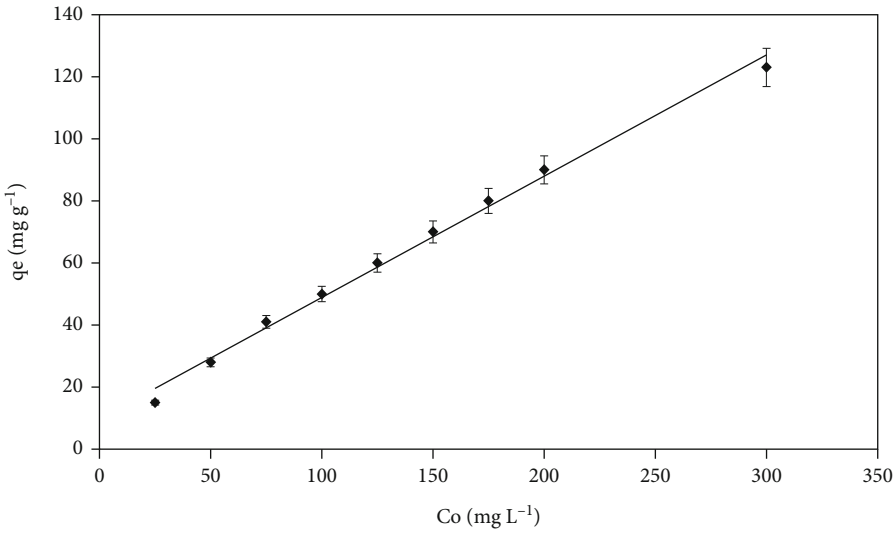

Figure 5: Influence of initial concentration on PSS (adsorbent dose: 0.05 g L^{-1}; room temperature; and contact time: 3 hrs).

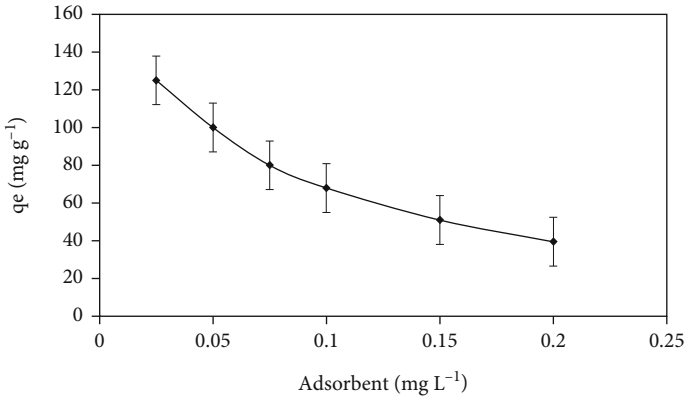

Figure 6: Graph of adsorbent (CV) effect on PSS (adsorbent dose: 0.05 g L^{-1}; room temperature; and contact time: 3 hrs).

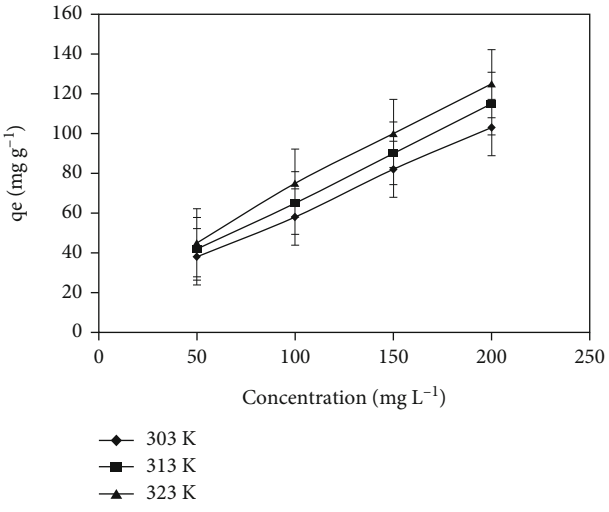

Figure 7: Graph of temperature effect on PSS (adsorbent dose: 0.05 g L^{-1}; room temperature; and contact time: 3 hrs).

which if the size of particles is large, more resistance to diffusion of mass transfer the interior particles would not be exposed for surface adsorption, subsequently resulting in lower adsorption of dye.

3.3. Isotherms of Adsorption. The interaction of the adsorbent and the adsorbate is important to understand the adsorption process mechanism. This is facilitated by fitting the data of adsorption to various isotherms of adsorption governed by different models. Tables 4, 5, 6, and 7 display the highest values for chi-square (χ^2), coefficient of correlation (R^2), peak adsorption capacity (Q_m), and other concerned parameters for the desired isotherms. The consideration in Langmuir isotherm is that the surface of adsorption is homogeneous with all points available for transaction with the adsorbate equally containing uniform energy [71]. The assumptions prescribed are for the case of adsorption in monolayer, where molecules of the adsorbate exhibit no transmission on the surface. The present study has predicted a maximum adsorption capacity (Q_m) of 204.79 mg g^{-1} Langmuir isotherm. Conversely, the experimental value is

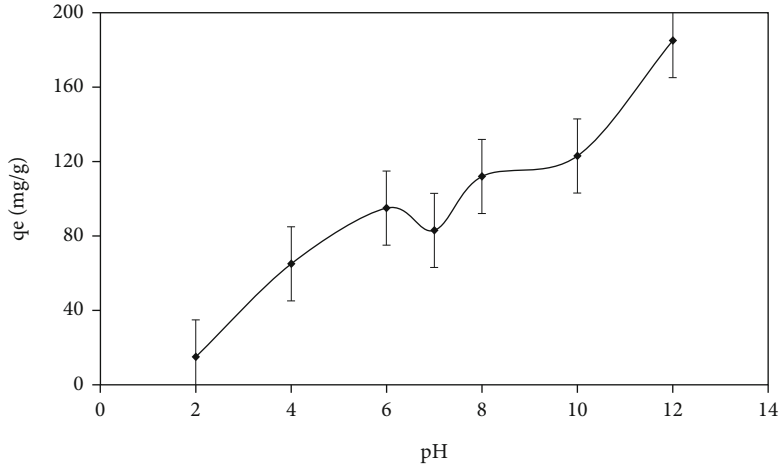

Figure 8: Graph of pH effect on CV (adsorbent dose: 0.05 g L^{-1}; room temperature; and contact time: 3 hrs).

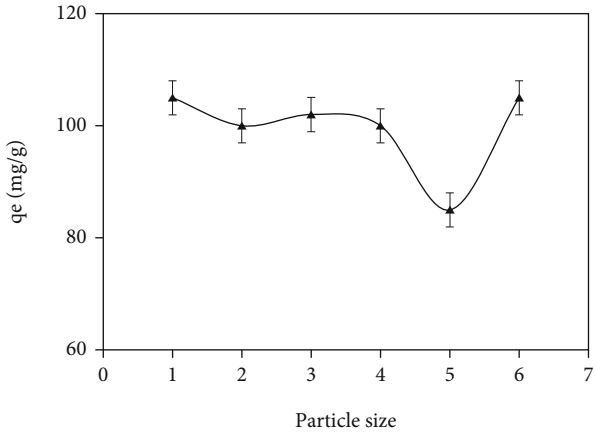

Figure 9: Graph of particle size effect on CV (adsorbent dose: 0.05 g L^{-1}; room temperature; and contact time: 3 hrs).

significantly different at 87.26 mg g^{-1}(Figure 10). Since the Langmuir isotherm is derived from thermodynamic principles, an important metric called the separation (R_L) can be predicted [72]. The separation factor is an indicator to access the adsorption system conditions based on the criteria linear ($R_L = 1$), favorable ($0 < R_L < 1$), unfavorable ($R_L > 1$), or irreversible ($R_L = 0$). In this work, for the concentration of 25–200 mg L^{-1}, the values obtained were 0.85 and 0.41, which indicates favorable adsorption of dye on PSS. As expected, a decrease in R_L with the higher initial dye concentration signifies more favorable adsorption with increased concentration.

Another proposed adsorption mechanism is that proposed by Freundlich. This isotherm assumes that heterogeneous adsorbate layers can be formed, and an empirical model can be used to describe this process [73]. The metric called the heterogeneity factor (n_F) can be estimated from the Freundlich isotherm. This classifies the adsorption mechanism to be chemisorption ($n_F < 1$), physisorption ($n_F > 1$), or linear ($n_F = 1$). This parameter can also be used to quickly identify if a process follows normal Langmuir isotherm $[(1/n_F) < 1]$ or cooperative adsorption $[(1/n_F) > 1]$. The current experimental investigation revealed the values of $n_F = 1.4$ and $1/n_F = 0.72$, which indicated adsorption to be physisorption, which concerns Langmuir isotherm. These Langmuir and Freundlich isotherms and the experimentally obtained data ($R^2 = 0.994$ and 0.998, respectively). The Tempkin isotherm uses a thermodynamic approach to explain multiple layers with possible interactions between them. This is in agreement with the Freundlich isotherm. The assumption used in the Tempkin isotherms specifies that the molecules in a covered layer lose the heat of adsorption linearly, and the distribution of maximum energy of adsorption is uniform [74]. The thermodynamic parameter constant b_T can be approximated from the Tempkin isotherm constant. This estimated value of b_T is used to tabulate adsorption heat value, $B = \mathrm{RT}/b_T$, where gas constant $R = 8.314\ \mathrm{J\,K^{-1}\,mol^{-1}}$ and the temperature T in kelvin [K]. The value of $B = 30.63\ \mathrm{J^{-1}\,mol}$ is low which substantiates that adsorption is a physical phenomenon. Figure 11 represents experimental data fit ($R^2 = 0.945$) which specifies that Tempkin isotherm elucidates the adsorption of dye onto the adsorbent. Most of the other isotherms are expanded forms of either the Langmuir or Freundlich isotherms. Jovanovic isotherm is an expanded form of Langmuir isotherm, [75] which describes a model considering a single layer and no crosswise interactions, but with an additional exponential term to compensate for experimental result deviations with that of Langmuir isotherm. Looking at Q_m, χ^2, and R^2 values, Langmuir appears to be a better fit than the Jovanovic model (Table 5).

Similarly, the Redlich–Peterson isotherm is an improvised fitting that uses a correction coefficient g to the Langmuir-Freundlich equations [76]. At ($g = 1$) and ($g = 0$), the equations represent Langmuir and Freundlich isotherm, respectively. The value of $g = 0.3$ obtained specifies the adsorption process tendency towards the Freundlich model. Sips isotherm is better to represent isotherms of combined Langmuir, and Freundlich is the Sips isotherm [77]. The Sips equation translates to Langmuir isotherm at increased adsorbate concentrations and reduced concentration contracts to the Freundlich

Table 4: Calculated parametric values of 2-parameter isotherms.

2-parameter isotherms									
Langmuir		Freundlich		Jovanovich		Tempkin		Harkins-Jura	
Qm	204.79	K_F	3.06	Qm	129.4	b_T	82.24	Ahj	1028.42
K_S	0.007	n_F	1.4	K_J	0.01	k_T	0.13	Bhj	2.16

Table 5: Statistical parametric values for 2-parameter isotherms.

Models	Langmuir	Freundlich	Jovanovic	Tempkin	Harkins-Jura
SSE	33.73	11.01	42.05	250.92	388.75
χ^2	0.83	0.28	1.11	7.04	18.3
R^2	0.994	0.998	0.992	0.945	0.931

Table 6: Calculated parametric values of 3-parameter isotherms.

3-parameter isotherms											
Redlich-Peterson		Toth		Radke-Prausnitz		Sips		Vieth-Sladek		Brouers-Sotolongo	
A_{RP}	30.06	Qm	400	Qm	5.13	Qm	400.86	Qm	31.15	Qm	500
B_{RP}	9.13	n_{T0}	0.63	K_{RP}	0.52	K_S	0.0015	K_{VS}	0.5751	K_{BS}	0.005
g	0.3	b_{T0}	31.05	M_{RP}	0.3	M_S	0.78	β_{VS}	0.47	α	0.774

Table 7: Statistical parametric values for 3-parameter isotherms.

Models	Redlich-Peterson	Toth	Radke-Prausnitz	Sips	Vieth-Sladek	Brouers-Sotolongo
SSE	11.002	21.73	10.83	13.96	7.84	17.75
χ^2	0.27	0.43	0.25	0.27	0.2	0.38
R^2	0.998	0.995	0.998	0.997	0.998	0.997

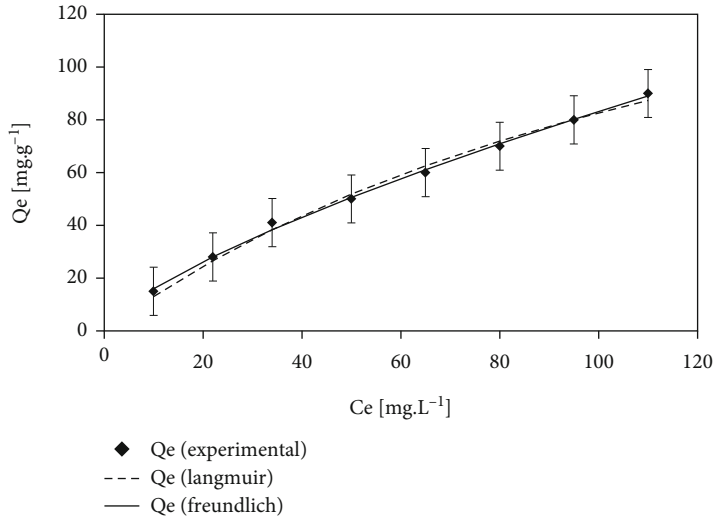

Figure 10: Adsorption data to Langmuir isotherm and Freundlich isotherm.

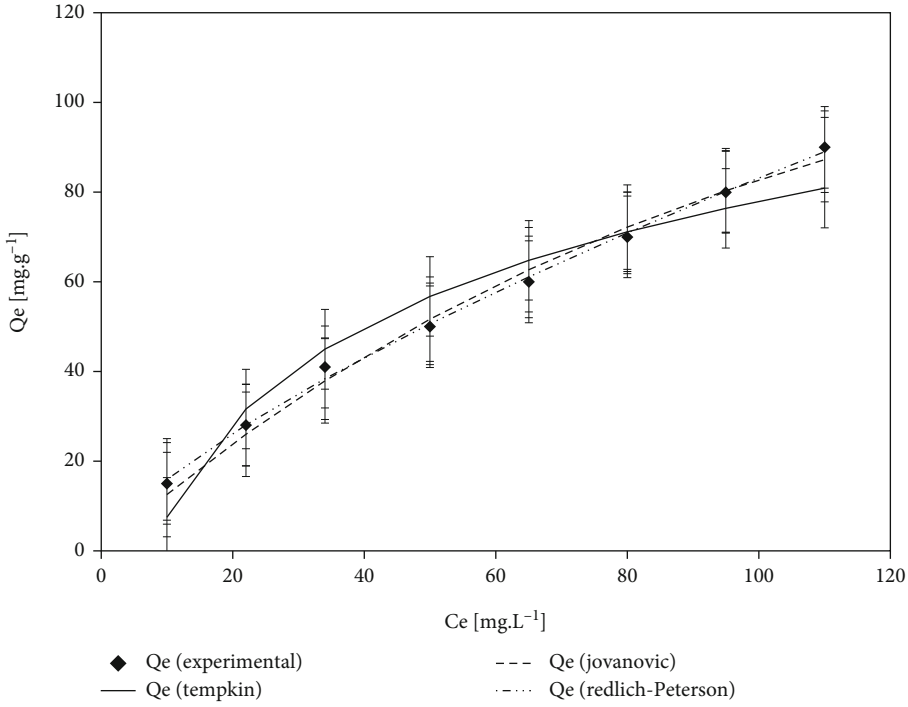

Figure 11: Adsorption data fitting to Jovanovic, Tempkin, and Redlich-Peterson models.

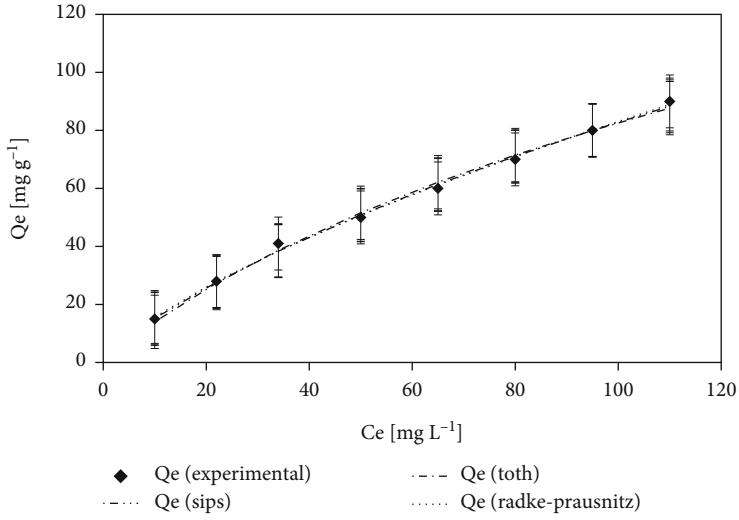

Figure 12: Adsorption data fitting to Sips, Toth, and Radke-Prausnitz isotherm.

equation. In this study, the Q_m value obtained for the Sips isotherm is 400.86 mg g^{-1}.

On the contrary, Radke-Prausnitz isotherm [78] predicted Q_m of 5.13 mg g^{-1} was obtained which was least near the experimentally obtained Q_m value. The fits of Sips isotherm ($R^2 = 0.997$), Radke-Prausnitz isotherm ($R^2 = 0.998$), and Toth isotherm ($R^2 = 0.995$). Another empirically determined isotherm model is the Toth isotherm [79]. The Toth isotherm tries to explain the heterogeneous adsorption systems by building on the Langmuir isotherm (Figure 12). The Jovanovic isotherm calculated $Q_m = 129.4$ mg g^{-1}, the nearest value to the experimental value. $Q_m = 31.15$ mg g^{-1} value was obtained for Vieth-Sladek model [80]. The fits of Vieth-Sladek ($R^2 = 0.998$), Brouers-Sotolongo ($R^2 = 0.997$), and Harkins-Jura ($R^2 = 0.931$) models to experimentally obtained values are depicted in Figure 13. The fits of Tempkin isotherm ($R^2 = 0.945$), Jovanovic model ($R^2 = 0.992$), and Redlich-Peterson model ($R^2 = 0.998$) are shown. Harkins-Jura isotherm [81] assumes multiple layers of adsorption of the adsorbent on a heterogeneously distributed porous adsorbate.

The adsorption process mechanism models studied are equations of higher order. The data fitting validation cannot be assured only by considering the R^2 value, a statistical

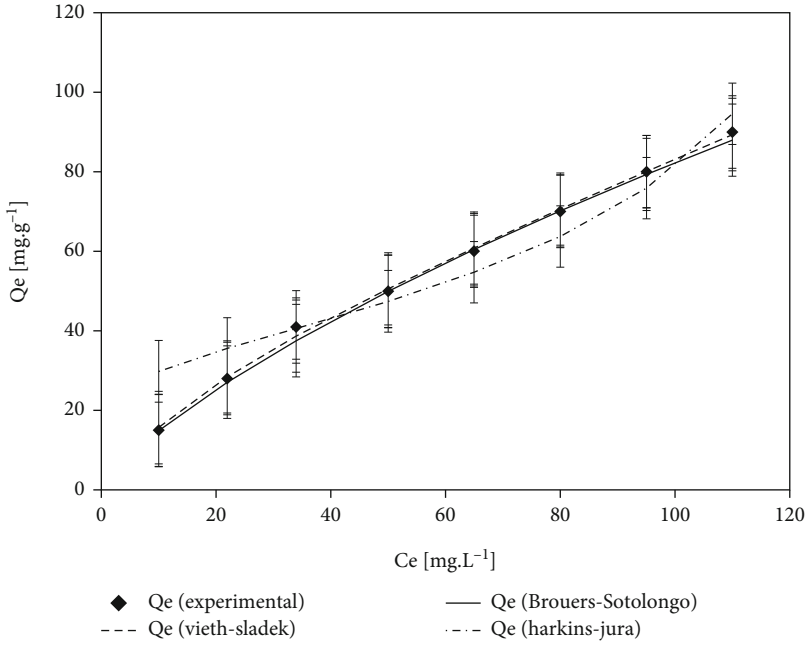

Figure 13: Adsorption data fitting to Vieth-Sladek, Brouers-Sotolongo, and Harkins-Jura models.

parameter compatible with linear models. Thus, the χ^2 values are used for accurate statistics. The χ^2 will be a small value if the model and experimental data are the same and a higher value for models that are not compatible with the data from experiments. The analysis of models and understanding of critical parameters (Q_m, χ^2, and R^2) makes it possible to arrange isotherms based on their capacity to predict the experimental behavior of the CV-PSS system. With respect to Q_m value (closest to actual value to farthest from actual value), Jovanovic > Langmuir > Vieth-Sladek > Sips > Toth > Radke-Prausnitz, whereas, based on χ^2 (descending order), Vieth-Sladek > Radke-Prausnitz > Sips > Redlich-Peterson > Freundlich > Brouers-Sotolongo > Toth > Langmuir > Jovanovic > Tempkin > Harkins-Jura.

3.4. Kinetics of Adsorption. CV concentration in water is critical in the study of kinetics. CV concentrations considered in the kinetic study were 50, 100, and 200 ppm. These studies show a similarity with the studies reported [22, 25]. By studying the kinetics at 303 K, 313 K, and 323 K temperatures, the variations in adsorption rate with temperature changes were understood. The nonlinear data analysis of the adsorption and desorption process kinetics was done by applying kinetic models, namely, the first-order pseudo model [82], second-order pseudo model [83], Avrami kinetic model [84], Weber-Morris intraparticle diffusion model [85], Dumwald-Wagner kinetic model [86], and film diffusion kinetic model [87]. The parameters approximated are presented in Tables 8 and 9. The second-order pseudo-kinetic model data and experimental data for R^2 and χ^2 are compatible as shown in Figures 14, 15, and 16 for 50 ppm, 100 ppm, and 200 ppm concentrations of CV. It is interesting to observe that the rate of adsorption at the very beginning of the process is very high and then slows down over time until it attains peak adsorption potential, becoming stagnant. It is predictable that with temperature rise, the adsorption potential (q_e) increases. It can be concluded from the results that the rate of the adsorption process is not limited.

The Avrami model equations were applied to describe the adsorption of CV onto PSS. The rates of adsorption are expressed as functions of initial CV concentration and duration of the adsorption process. The experimental and theoretical results' conformity is established from calculated values of q_e, and R^2 is represented in Table 9. It was observed that the model would be fit only if the factionary number (n_{AV}) as obtained from the prediction of adsorption processes was equal to 1 in all cases. The equilibrium adsorption capacities (q_e) predicted were the same as that of pseudo-second-order models and quite near experimentally obtained results. This indicated that CV adsorption kinetics onto PSS was associated with second-order pseudo kinetics concerning time irrespective of the changes in solution initial CV concentration.

The information obtained reveals that the process of adsorption takes place in several steps: firstly, the molecular diffusion of solute from solution to the surface of solid, and secondly, solute molecules diffuse to the PSS pores. To understand solute movement, the data were analyzed to study the effects of diffusion.

The Weber-Morris model (Figure 17) is routinely used to describe molecular diffusion and specifies that at $t^{½}$ the solute rise varies conversely to the duration of contact (t). Thus, the q_t vs. $t½$ shows a straight line that passes through the origin with a slope (k_{int}) which is a constant rate of diffusion. However, only one mechanism cannot control the adsorption kinetics. It is evident from the experimental

Table 8: Adsorption kinetic model parameters from experimental and theoretical studies.

Initial concentration	Temp	Qe_{expt}	Pseudo-first order				Pseudo-second order				Avrami				
[ppm]	[K]	$[mg.g^{-1}]$	Qe_{pred} $[mg.g^{-1}]$	k_1	R^2	χ^2	Qe_{pred} $[mg.g^{-1}]$	k_2	R^2	χ^2	Qe_{pred} $[mg.g^{-1}]$	k_{AV}	n_{AV}	R^2	χ^2
	303	38	30.07	0.080	0.84	3.09	35.04	0.003	0.92	1.24	30.07	0.080	1	0.84	3.09
50	313	42	36.11	0.116	0.88	1.70	40.74	0.004	0.98	0.28	36.11	0.116	1	0.88	1.70
	323	45	39.36	0.106	0.88	2.47	44.40	0.003	0.93	1.15	39.36	0.106	1	0.88	2.47
	303	58	51.30	0.062	0.95	3.12	61.18	0.001	0.98	1.27	51.30	0.062	1	0.95	3.12
100	313	65	57.90	0.061	0.94	4.65	68.75	0.001	0.95	2.62	57.90	0.061	1	0.94	4.65
	323	75	64.58	0.066	0.93	4.54	76.31	0.001	0.97	1.47	64.58	0.066	1	0.93	4.54
	303	103	92.43	0.078	0.86	10.31	106.30	0.001	0.92	4.42	92.43	0.078	1	0.84	10.31
200	313	115	93.60	0.113	0.81	7.21	105.72	0.002	0.94	2.14	93.60	0.113	1	0.88	7.21
	323	125	110.47	0.098	0.95	3.90	125.59	0.001	0.98	1.04	110.47	0.098	1	0.88	3.90

Table 9: Diffusion model parameters.

Initial concentration	Temp	Film diffusion model		Weber-Morris model		Dumwald-Wagner	
[ppm]	[K]	R [min^{-1}]	R^2	k_{ist} [$mg/g.s^{-0.5}$]	R^2	K [min^{-1}]	R^2
	303	0.0209	0.98	2.638	0.98	0.017042	0.98
50	313	0.0234	0.89	2.979	0.9	0.020036	0.92
	323	0.0233	0.87	3.16	0.87	0.019806	0.9
	303	0.0302	0.99	5.15	0.96	0.022569	0.99
100	313	0.0309	0.98	5.46	0.93	0.020497	0.95
	323	0.0266	0.99	5.99	0.97	0.020266	0.99
	303	0.0327	0.99	7.72	0.96	0.028788	0.99
200	313	0.0199	0.95	7.26	0.95	0.016812	0.97
	323	0.0228	0.82	8.89	0.88	0.024872	0.81

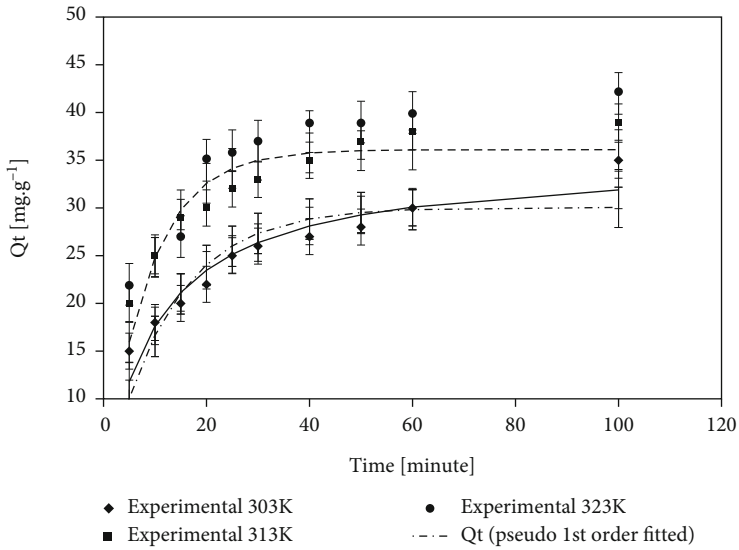

Figure 14: 50 ppm CV concentration on PSS kinetic model fit at temperatures 303 K, 313 K, and 323 K.

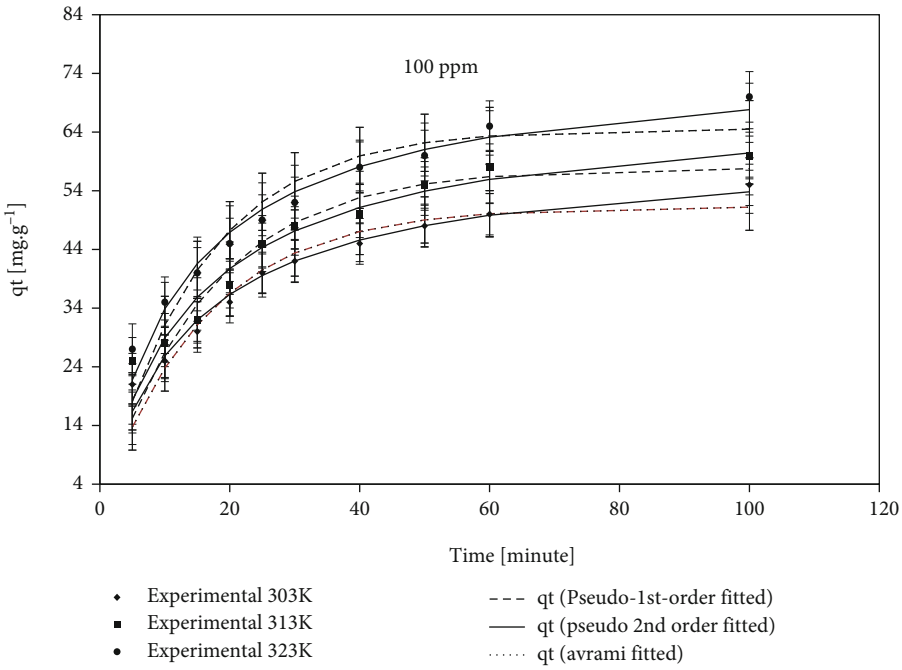

Figure 15: 100 ppm CV concentration on PSS kinetic model fit at temperatures 303 K, 313 K and 323 K.

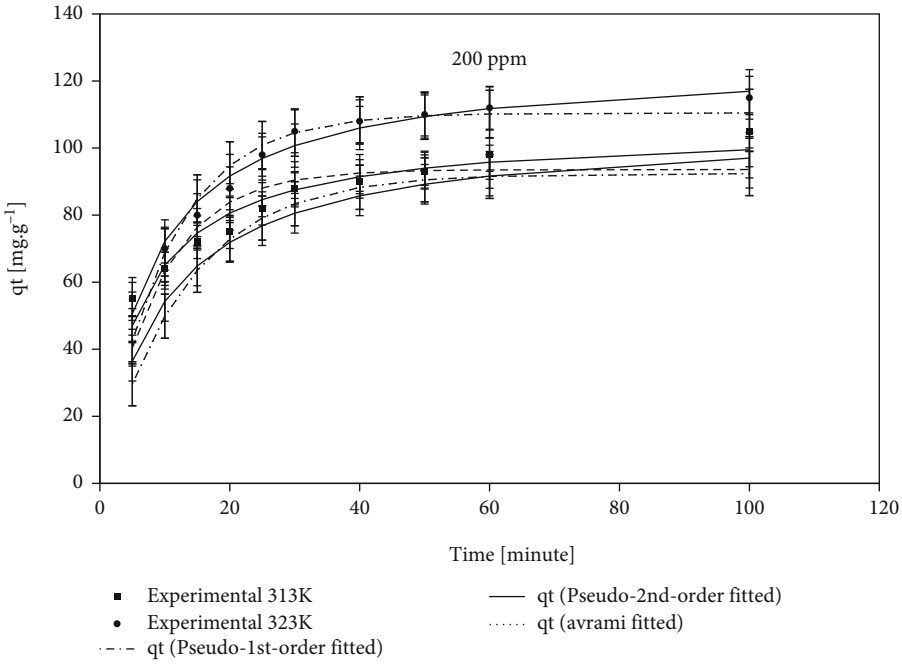

Figure 16: 200 ppm CV concentration on PSS kinetic model fit at temperatures 303 K, 313 K and 323 K.

results that linear variation exists in multiple ayers for all solute concentrations. At lower temperatures and concentrations of 50 ppm, the adsorption rate spikes, followed by a sudden linear rate change, which further stabilizes relative to time. However, the adsorption rate appears to be linear at higher temperatures. At the solute concentration of 200 ppm, it has been noted that the adsorption rate changes are less apparent. It can be witnessed from Figure 18 that the fit of the film diffusion model for higher temperatures displays good compatibility with the diffusion model at higher R^2 and χ^2 and provides constant R |, tabulated in Table 9. The conclusion withdrawn from these observations is that at increased temperatures, the process rate is negligibly influenced by diffusion limits. Thus, diffusion limits the process rate. Initially, the solute is absorbed to form a film onto the particle surface, which resists diffusion later and

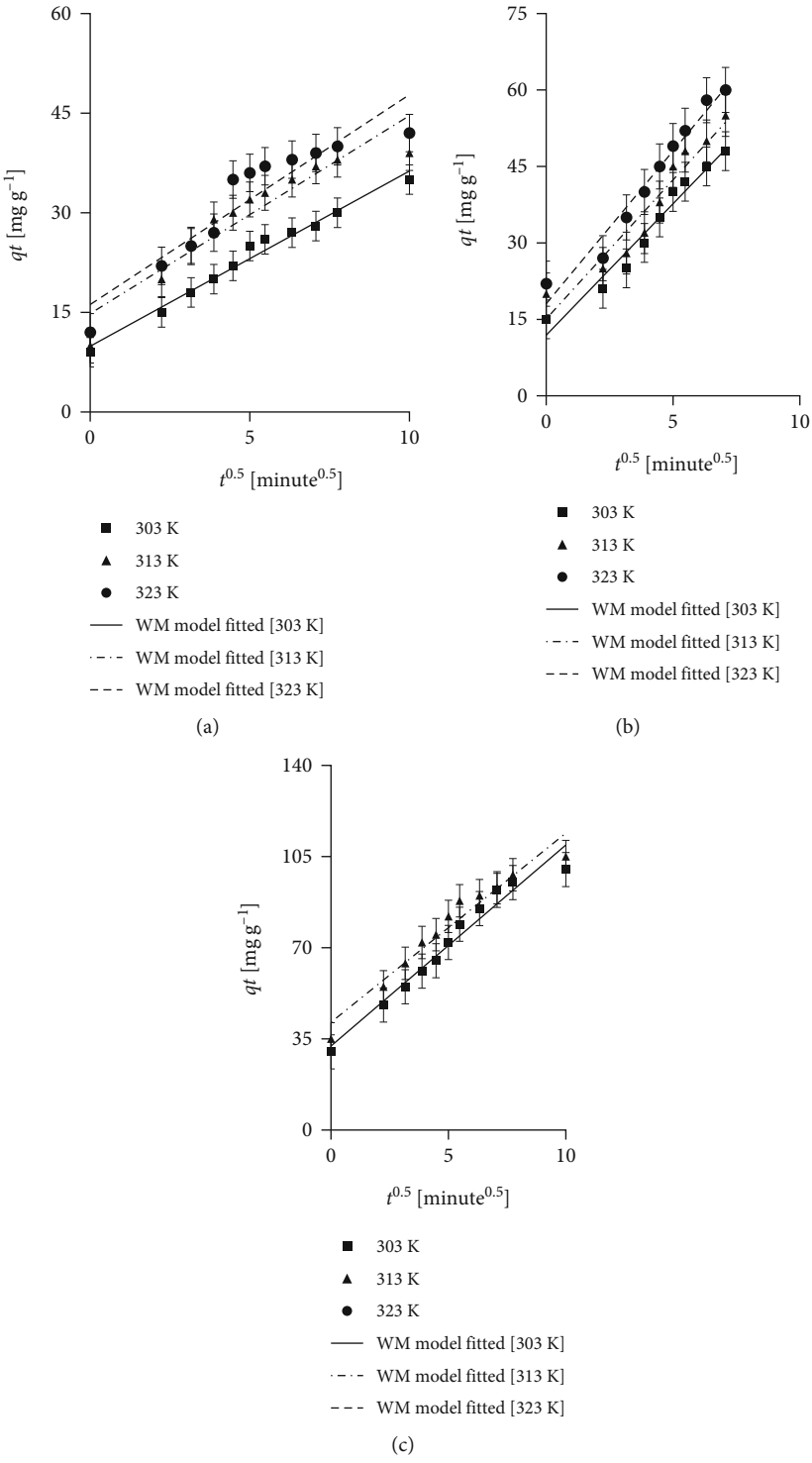

Figure 17: Data kinetics fit of Weber- Morris model with CV concentrations of (a) 50 ppm, (b) 100 ppm, and (c) 200 ppm.

thus changes the adsorption rates. The Dumwald-Wagner model (Figure 19) has also been used to calculate the actual value of K, including the correction factor for effects of diffusion (Table 9).

3.5. Effects of Thermodynamics of Adsorption. The free energy = ΔG^0 (kJ mol^{-1}), enthalpy change = ΔH^0 (kJ mol^{-1}), and entropy = ΔS^0 (J mol^{-1} K^{-1}), which are thermodynamic factors of adsorption calculation, were done using

$$\log\left(\frac{q_e m}{C_e}\right) = \left(\frac{\Delta S^\circ}{2.303R}\right) + \left(\frac{-\Delta H^\circ}{2.303\mathrm{RT}}\right), \tag{4}$$

$$\Delta G^0 = \Delta H^0 - T\Delta S^0, \tag{5}$$

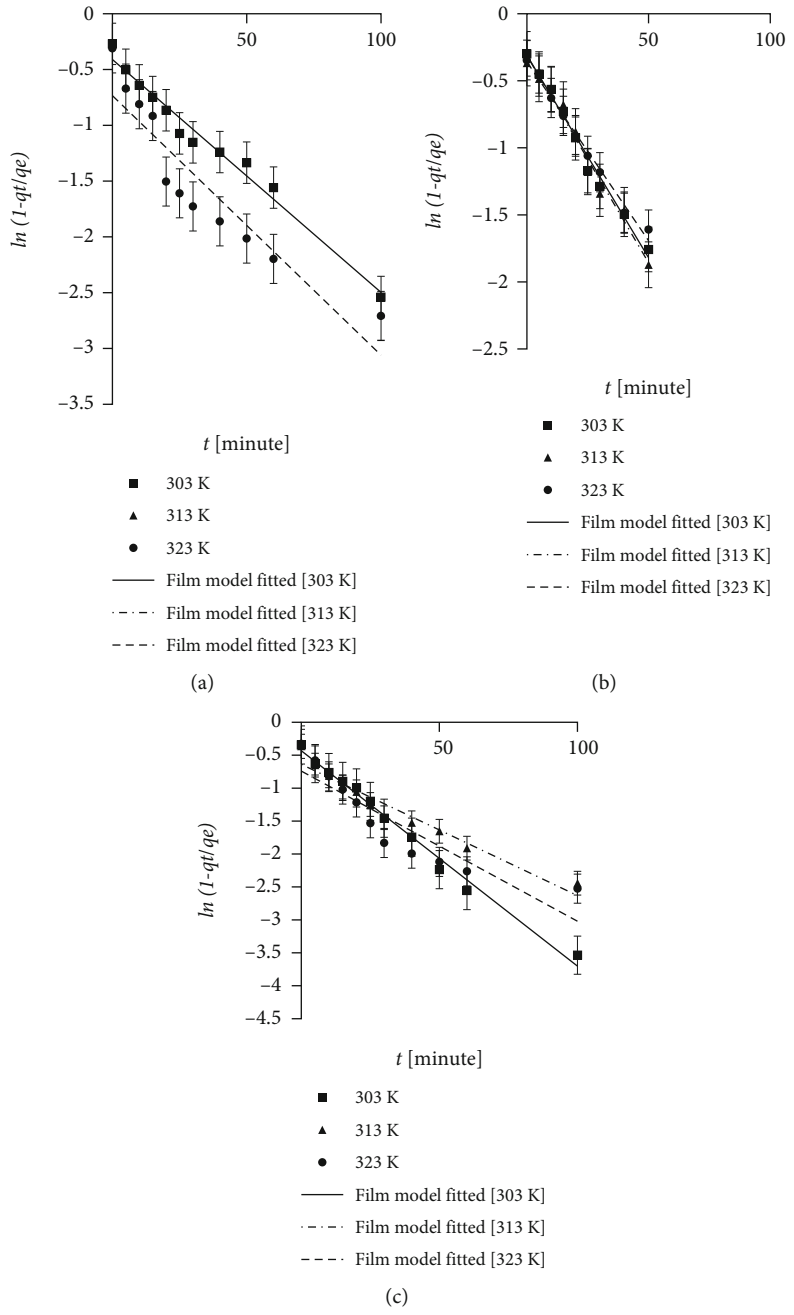

Figure 18: Data kinetics fit of Film diffusion model with CV concentrations of (a) 50 ppm, (b) 100 ppm, and (c) 200 ppm.

where m is the adsorbent quantity (g/L), C_e is the equilibrium dye concentration ($mg\,L^{-1}$), q_e is the dye adsorbed per unit adsorbent mass at equilibrium ($mg\,g^{-1}$), q_e/C_e is the adsorption affinity, R is the gas constant ($8.314\,J^{-1}mol^{-1}K$), and temperature is T (K). The plot of log ($q_e m/C_e$) vs. $1/T$, provides the values of ΔH° and ΔS°; after that from Equation (5), ΔG° is obtained. Table 10 is the collection of thermodynamic parameters.

The positive ΔH° values confirm that the adsorption process is endothermic. The enthalpy change for adsorption chemical reaction is usually $>200\,kJ\,mol^{-1}$, and the process capability enhances with temperature rise. The positive ΔS° indicates more CV-adsorbent affinity and more volatility at the solution surface. The negative ΔG° for all temperature attributes reduction in free energy and adsorption of dye CV onto the PSS surface. This establishes the practicability and impulsiveness of adsorption. ΔG° decreased with a rise in temperature, which indicates an enhancement in the absorption process.

3.6. Adsorbent Regeneration and Its Cost Analysis. The adsorbent regeneration facilitates biomass reuse and recovery of adsorbed materials. The process cost and solvent price are more expensive than the adsorbents used. Hence, it is

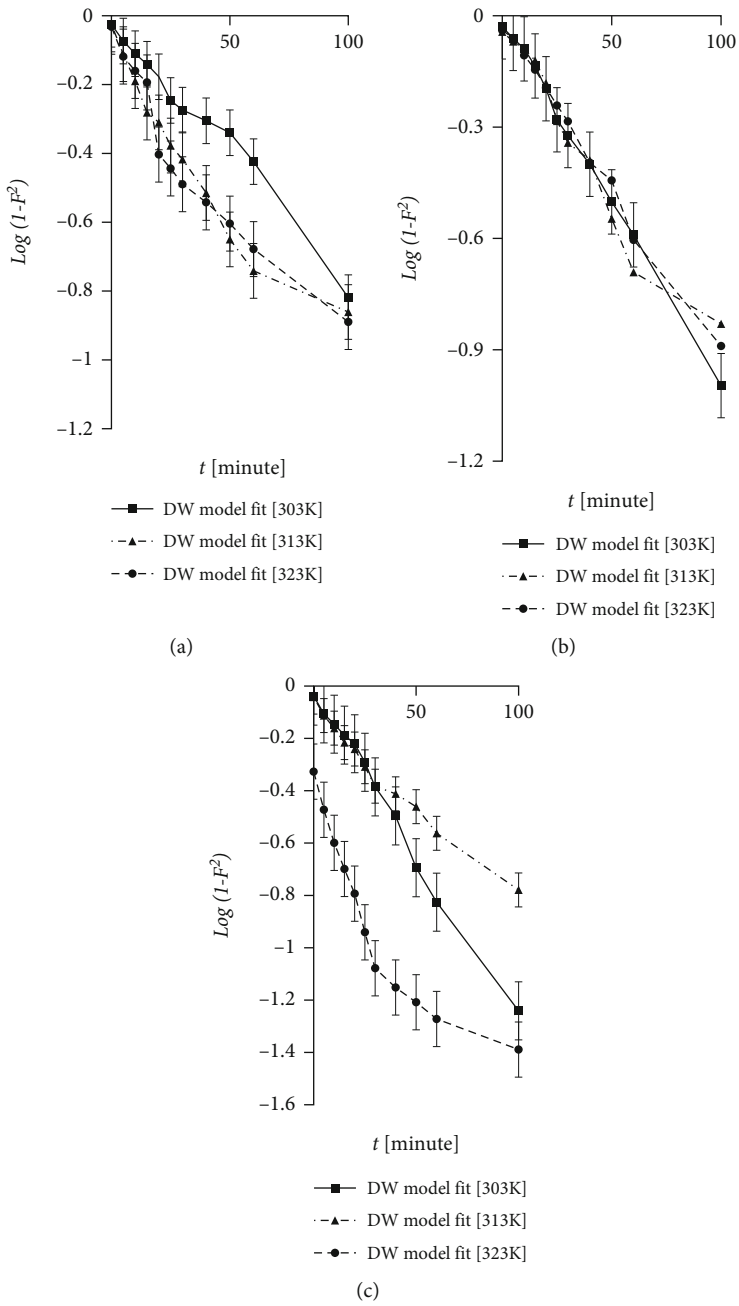

Figure 19: Data kinetics fit of Dumwald-Wagner model with CV concentrations of (a) 50 ppm, (b) 100 ppm, and (c) 200 ppm.

Table 10: Calculated thermodynamic parameters.

Thermodynamic parameters Concentration (mg L^{-1})	ΔH^0 (kJ Mol^{-1})	ΔS^0 ($J^{-1}mol^{-1}K$)	$-\Delta G^0$ (kJ Mol^{-1})		
			303 K	313 K	323 K
50	42.267	162.308	6.912	8.533	10.158
100	31.234	118.83	4.771	5.959	7.147
150	20.424	82.202	4.483	5.305	6.127
200	18.289	74.23	4.204	4.946	5.689

not an advisable strategy. Apart from this, the E-factor is increased, which is linked to environmental contamination. The overall consideration of these aspects has led to the proposition of a novel method to incorporate waste excreted by dye adsorbed biosorbent as filler material to fabricate thermosets and thermoplastics.

The proposed method of adsorption of a dye on the nutraceutical industrial pepper seed spent was extended to the dye adsorption in the textile industrial effluent. Absorption spectra of industrial effluent IE sample solution with and without the CV dye were recorded. Using the Beer-Lambert law, the absorbance of CV was recorded at different concentrations. It was observed that the absorbance was proportional to the amount of material present. The results indicated that 0.5 g of NIPSS was sufficient for the experiments designed. The findings suggest that this experiment as a proof-of-concept can be explored further and applied to industries on a larger scale.

4. Conclusions

The first-ever study on the use of PSS, a nutraceutical industrial spent, was carried out to develop a green and low-cost biosorbent with a motto to remediate toxic dye CV. The peak value of adsorption obtained was $Q_m = 87.26\,\mathrm{mg\,g^{-1}}$, which was close to that obtained by the Jovanovic isotherm ($Q_m = 129.4/\mathrm{g}$) with the correlation coefficient (R^2) of 0.945. In contrast, Vieth–Sladek isotherm gave maximum fitting isotherm ($\chi^2 = 0.2$). The experiment results fit the kinetic model of pseudo-second order, which the Avrami model further verified. However, the considerable effect of film diffusion and intraparticle diffusion was revealed. The adsorption was observed to be a spontaneous and endothermic process. The reduced ΔH^0 value is attributed to the physical predominance of the process. The FTIR spectrum analysis assured the absorption of CV on PSS. Based on this, the interaction mechanisms that occur in the CV-PSS system have been discussed. It can be concluded that the PSS adsorbent is a fast and efficient means for the removal of dye CV from the solution, which can further be used in alternate structural materials or as fillers when preparing thermoplastics and thermosets adapting works previously performed in our previous studies.

Data Availability

The data used to support the findings of this study are available from the corresponding author upon request.

Conflicts of Interest

The authors declare that they have no conflicts of interest.

Authors' Contributions

The authors confirm their contributions to the present work as follows: RS, SNT, and UTS came up with the concept and methodology. Validation and approval of the work were carried out by TMYK and IM; formal work and analysis were done by RS; and concept and original draft preparation were carried out by AAS. Further review and editing was done by RS, KS, MAK, SJ, and HCAM. All the authors have read and agreed to the published version of the manuscript.

Acknowledgments

The authors extend his appreciation to the Deanship of Scientific Research at King Khalid University for funding this work through research groups program 1/214/43.

References

[1] K. Kadirvelu, M. Kavipriya, C. Karthika, M. Radhika, N. Vennilamani, and S. Pattabhi, "Utilization of various agricultural wastes for activated carbon preparation and application for the removal of dyes and metal ions from aqueous solutions," *Bioresource Technology*, vol. 87, no. 1, pp. 129–132, 2003.

[2] S. Patil, V. Deshmukh, S. Renukdas, and N. Pate, "Kinetics of adsorption of crystal violet from aqueous solutions using different natural materials," *International Journal of Environmental Sciences*, vol. 1, no. 6, pp. 1116–1134, 2011.

[3] S. Chowdhury, R. Mishra, P. Saha, and P. Kushwaha, "Adsorption thermodynamics, kinetics and isosteric heat of adsorption of malachite green onto chemically modified rice husk," *Desalination*, vol. 265, no. 1-3, pp. 159–168, 2011.

[4] Y. Wong, Y. S. Szeto, W. H. Cheung, and G. McKay, "Adsorption of acid dyes on chitosan—equilibrium isotherm analyses," *Process Biochemistry*, vol. 39, no. 6, pp. 695–704, 2004.

[5] T. K. Sen, S. Afroze, and H. Ang, "Equilibrium, kinetics and mechanism of removal of methylene blue from aqueous solution by adsorption onto pine cone biomass of Pinus radiata," *Water, Air, & Soil Pollution*, vol. 218, no. 1-4, pp. 499–515, 2011.

[6] M. T. Yagub, T. K. Sen, and H. M. Ang, "Equilibrium, kinetics, and thermodynamics of methylene blue adsorption by pine tree leaves," *Water, Air, & Soil Pollution*, vol. 223, no. 8, pp. 5267–5282, 2012.

[7] S. K. Bajpai and A. Jain, "Equilibrium and thermodynamic studies for adsorption of crystal violet onto spent tea leaves (STL)," *Water*, vol. 4, pp. 52–71, 2012.

[8] D. Jirekar, P. Ghumare, and F. Mazahar, "Kinetics and isotherm studies on crystal violet dye adsorption onto black gram seed husk," *International Journal of ChemTech Research*, vol. 7, no. 1, pp. 427–434, 2015.

[9] A. Durán, J. Monteagudo, and E. Amores, "Solar photo-fenton degradation of reactive blue 4 in a CPC reactor," *Applied Catalysis B: Environmental*, vol. 80, no. 1-2, pp. 42–50, 2008.

[10] J. Sun, L. Qiao, S. Sun, and G. Wang, "Photocatalytic degradation of orange G on nitrogen-doped TiO_2 catalysts under visible light and sunlight irradiation," *Journal of Hazardous Materials*, vol. 155, no. 1-2, pp. 312–319, 2008.

[11] G. Sudarjanto, B. Keller-Lehmann, and J. Keller, "Optimization of integrated chemical-biological degradation of a reactive azo dye using response surface methodology," *Journal of Hazardous Materials*, vol. 138, no. 1, pp. 160–168, 2006.

[12] L. Fan, Y. Zhou, W. Yang, G. Chen, and F. Yang, "Electrochemical degradation of aqueous solution of amaranth azo dye on ACF under potentiostatic model," *Dyes and Pigments*, vol. 76, no. 2, pp. 440–446, 2008.

[13] B. H. Hameed, "Spent tea leaves: a new non-conventional and low-cost adsorbent for removal of basic dye from aqueous solutions," *Journal of Hazardous Materials*, vol. 161, no. 2-3, pp. 753–759, 2009.

[14] D. Balarak, T. J. al-Musawi, I. A. Mohammed, and H. Abasizadeh, "The eradication of reactive black 5 dye liquid wastes using Azolla filiculoides aquatic fern as a good and an economical biosorption agent," *SN Applied Sciences*, vol. 2, no. 6, p. 1015, 2020.

[15] D. Balarak, M. Zafariyan, C. A. Igwegbe, K. K. Onyechi, and J. O. Ighalo, "Adsorption of acid blue 92 dye from aqueous solutions by single-walled carbon nanotubes: isothermal, kinetic, and thermodynamic studies," *Environmental Processes*, vol. 8, no. 2, pp. 869–888, 2021.

[16] T. J. Al-Musawi, N. Mengelizadeh, O. Al Rawi, and D. Balarak, "Capacity and modeling of acid blue 113 dye adsorption onto chitosan magnetized by Fe2O3 nanoparticles," *Journal of Polymers and the Environment*, vol. 30, no. 1, pp. 344–359, 2022.

[17] M. Sillanpää, A. H. Mahvi, D. Balarak, and A. D. Khatibi, "Adsorption of acid orange 7 dyes from aqueous solution using polypyrrole/nanosilica composite: experimental and modelling," *International Journal of Environmental Analytical Chemistry*, vol. 101, pp. 1–18, 2021.

[18] S. Senthilkumaar, P. Kalaamani, and C. Subburaam, "Liquid phase adsorption of crystal violet onto activated carbons derived from male flowers of coconut tree," *Journal of Hazardous Materials*, vol. 136, no. 3, pp. 800–808, 2006.

[19] S. Karaca, A. Gürses, M. Açıkyıldız, and M. Ejder (Korucu), "Adsorption of cationic dye from aqueous solutions by activated carbon," *Microporous and Mesoporous Materials*, vol. 115, no. 3, pp. 376–382, 2008.

[20] J. Mahadev, S. P. Hosamani, and S. A. Ahmed, "Statistical multivariate analysis of lakes water quality parameters in Mysore, Karnataka, India," *World Applied Sciences Journal*, vol. 8, no. 11, pp. 1370–1380, 2010.

[21] M. A. Syed, S. Akhtar, and A. A. Syed, "Studies on the physicomechanical, thermal, and morphological behaviors of high density polyethylene/coleus spent green composites," *Journal of Applied Polymer Science*, vol. 119, no. 4, pp. 1889–1895, 2011.

[22] R. Ahmad and R. Kumar, "Adsorption studies of hazardous malachite green onto treated ginger waste," *Journal of Environmental Management*, vol. 91, no. 4, pp. 1032–1038, 2010.

[23] A. Mittal, L. Krishnan, and V. Gupta, "Removal and recovery of malachite green from wastewater using an agricultural waste material, de-oiled soya," *Separation and Purification Technology*, vol. 43, no. 2, pp. 125–133, 2005.

[24] K. V. Kumar, "Optimum sorption isotherm by linear and nonlinear methods for malachite green onto lemon peel," *Dyes and Pigments*, vol. 74, no. 3, pp. 595–597, 2007.

[25] B. Hameed and M. El-Khaiary, "Malachite green adsorption by rattan sawdust: isotherm, kinetic and mechanism modeling," *Journal of Hazardous Materials*, vol. 159, no. 2-3, pp. 574–579, 2008.

[26] P. Saha, S. Chowdhury, S. Gupta, I. Kumar, and R. Kumar, "Assessment on the removal of malachite green using tamarind fruit shell as biosorbent," *Water*, vol. 38, no. 5-6, pp. 437–445, 2010.

[27] G. Sonawane and V. Shrivastava, "Kinetics of decolourization of malachite green from aqueous medium by maize cob (Zea maize): an agricultural solid waste," *Desalination*, vol. 247, no. 1-3, pp. 430–441, 2009.

[28] S. Chowdhury and P. Saha, "Sea shell powder as a new adsorbent to remove basic green 4 (malachite green) from aqueous solutions: equilibrium, kinetic and thermodynamic studies," *Chemical Engineering Journal*, vol. 164, no. 1, pp. 168–177, 2010.

[29] C. T. Weber, G. C. Collazzo, M. A. Mazutti, E. L. Foletto, and G. L. Dotto, "Removal of hazardous pharmaceutical dyes by adsorption onto papaya seeds," *Water Science and Technology*, vol. 70, no. 1, pp. 102–107, 2014.

[30] C. Namasivayam, M. Dinesh Kumar, K. Selvi, R. Ashruffunissa Begum, T. Vanathi, and R. T. Yamuna, "'Waste' coir pith—a potential biomass for the treatment of dyeing wastewaters," *Biomass and Bioenergy*, vol. 21, no. 6, pp. 477–483, 2001.

[31] Y. Özdemir, M. Doğan, and M. Alkan, "Adsorption of cationic dyes from aqueous solutions by sepiolite," *Microporous and Mesoporous Materials*, vol. 96, no. 1-3, pp. 419–427, 2006.

[32] S. Khattri and M. Singh, "Colour removal from dye wastewater using sugar cane dust as an adsorbent," *Adsorption Science & Technology*, vol. 17, no. 4, pp. 269–282, 1999.

[33] H. Ali and S. K. Muhammad, "Biosorption of crystal violet from water on leaf biomass of Calotropis procera," *Journal of Environmental Science and Technology*, vol. 1, no. 3, pp. 143–150, 2008.

[34] S. Khattri and M. Singh, "Colour removal from synthetic dye wastewater using a bioadsorbent," *Water, Air, and Soil Pollution*, vol. 120, no. 3/4, pp. 283–294, 2000.

[35] H. Parab, M. Sudersanan, N. Shenoy, T. Pathare, and B. Vaze, "Use of agro-industrial wastes for removal of basic dyes from aqueous solutions," *Water*, vol. 37, no. 12, pp. 963–969, 2009.

[36] K. Bharathi and S. Ramesh, "Biosorption of crystal violet from aqueous solution by *Citrullus lanatus* (watermelon) rind," *Journal of Environmental Research and Development*, vol. 7, no. 1A, pp. 321–329, 2012.

[37] R. Dhodapkar, N. N. Rao, S. P. Pande, T. Nandy, and S. Devotta, "Adsorption of cationic dyes on Jalshakti®, super absorbent polymer and photocatalytic regeneration of the adsorbent," *Reactive and Functional Polymers*, vol. 67, no. 6, pp. 540–548, 2007.

[38] G. Annadurai, R.-S. Juang, and D.-J. Lee, "Use of cellulose-based wastes for adsorption of dyes from aqueous solutions," *Journal of Hazardous Materials*, vol. 92, no. 3, pp. 263–274, 2002.

[39] S. Jain and R. V. Jayaram, "Removal of basic dyes from aqueous solution by low-cost adsorbent: wood apple shell (*Feronia acidissima*)," *Desalination*, vol. 250, no. 3, pp. 921–927, 2010.

[40] I. D. Mall, V. C. Srivastava, and N. K. Agarwal, "Removal of orange-G and methyl violet dyes by adsorption onto bagasse fly ash—kinetic study and equilibrium isotherm analyses," *Dyes and Pigments*, vol. 69, no. 3, pp. 210–223, 2006.

[41] K. Porkodi and K. V. Kumar, "Equilibrium, kinetics and mechanism modeling and simulation of basic and acid dyes sorption onto jute fiber carbon: eosin yellow, malachite green and crystal violet single component systems," *Journal of Hazardous Materials*, vol. 143, no. 1-2, pp. 311–327, 2007.

[42] R. Ahmad, "Studies on adsorption of crystal violet dye from aqueous solution onto coniferous pinus bark powder (CPBP)," *Journal of Hazardous Materials*, vol. 171, no. 1-3, pp. 767–773, 2009.

[43] C. H. Wang, C. R. Chen, J. J. Wu, L. Y. Wang, C. M. J. Chang, and W. J. Ho, "Designing supercritical carbon dioxide extraction of rice bran oil that contain oryzanols using response surface methodology," *Journal of Separation Science*, vol. 31, no. 8, pp. 1399–1407, 2008.

[44] P. Saha, S. Das, S. A. Khanom, L. Islam, S. Begum, and S. Parveen, "Nutritional & microbiological quality assessment of dehydrated jackfruit (Artocarpusheterophyllus) seed powder," *Octa Journal of Biosciences*, vol. 4, no. 2, 2016.

[45] R. Kumar and R. Ahmad, "Biosorption of hazardous crystal violet dye from aqueous solution onto treated ginger waste (TGW)," *Desalination*, vol. 265, no. 1-3, pp. 112–118, 2011.

[46] J. Wang, B. Sun, Y. Cao, Y. Tian, and X. Li, "Optimisation of ultrasound-assisted extraction of phenolic compounds from wheat bran," *Food Chemistry*, vol. 106, no. 2, pp. 804–810, 2008.

[47] F. Atmani, A. Bensmaili, and N. Mezenner, "Synthetic textile effluent removal by skin almonds waste," *Journal of Environmental Science and Technology*, vol. 2, no. 4, pp. 153–169, 2009.

[48] R. A. Sheldon, "Organic synthesis-past, present and future," *Chemistry and Industry*, vol. 23, pp. 903–906, 1992.

[49] S. Pashaei, S. Hosseinzadeh, and A. A. Syed, "Studies on coconut shell powder and crysnanoclay incorporated acrylonitrile-butadiene rubber/ styrene butadiene rubber (NBR/SBR) green nanocomposites," *Polymer Composites*, vol. 38, no. 4, pp. 727–735, 2017.

[50] S. Pashaei, Siddaramaiah, and A. A. Syed, "Investigation on mechanical, thermal and morphological behaviors of turmeric spent incorporated vinyl ester green composites," *Polymer-Plastics Technology and Engineering*, vol. 50, no. 12, pp. 1187–1198, 2011.

[51] M. A. Syed and A. A. Syed, "Development of a new inexpensive green thermoplastic composite and evaluation of its physico-mechanical and wear properties," *Materials & Design*, vol. 36, pp. 421–427, 2012.

[52] M. A. Syed, Siddaramaiah, B. Suresha, and A. A. Syed, "Mechanical and abrasive wear behavior of coleus spent filled unsaturated polyester/polymethyl methacrylate semi interpenetrating polymer network composites," *Journal of Composite Materials*, vol. 43, no. 21, pp. 2387–2400, 2009.

[53] P. K. Papegowda and A. A. Syed, "Isotherm, kinetic and thermodynamic studies on the removal of methylene blue dye from aqueous solution using saw palmetto spent," *International Journal of Environmental Research*, vol. 11, no. 1, pp. 91–98, 2017.

[54] R. Sulthana, S. N. Taqui, F. Zameer, U. T. Syed, and A. A. Syed, "Adsorption of ethidium bromide from aqueous solution onto nutraceutical industrial fennel seed spent: kinetics and thermodynamics modeling studies," *International Journal of Phytoremediation*, vol. 20, no. 11, pp. 1075–1086, 2018.

[55] M. A. H. Allah, S. N. Taqui, U. T. Syed, and A. A. Syed, "Development of sustainable acid blue 113 dye adsorption system using nutraceutical industrial Tribulus terrestris spent," *SN Applied Sciences*, vol. 1, no. 4, pp. 1–18, 2019.

[56] S. N. Taqui, M. Cs, M. S. Goodarzi et al., "Sustainable adsorption method for the remediation of crystal violet dye using nutraceutical industrial fenugreek seed spent," *Applied Sciences*, vol. 11, no. 16, p. 7635, 2021.

[57] S. N. Taqui, M. Cs, B. A. Khatoon et al., "Sustainable adsorption method for the remediation of malachite green dye using nutraceutical industrial fenugreek seed spent," *Biomass Conversion and Biorefinery*, pp. 1–12, 2021.

[58] N. T. Syed, Y. Rosiyah, H. Aziz, N. Nayan, and A. S. Akheel, "Adsorption of acid blue 113 from aqueous solution onto nutraceutical industrial coriander seed spent: isotherm, kinetics, thermodynamics and modeling studies," *Desalination and Water Treatment*, vol. 153, pp. 321–337, 2019.

[59] S. N. Taqui, R. Yahya, A. Hassan, F. Khanum, and A. A. Syed, "Valorization of nutraceutical industrial coriander seed spent by the process of sustainable adsorption system of acid black 52 from aqueous solution," *International Journal of Environmental Research*, vol. 13, no. 4, pp. 639–659, 2019.

[60] S. N. Taqui, R. Yahya, A. Hassan, N. Nayak, and A. A. Syed, "A novel sustainable design to develop polypropylene and unsaturated polyester resin polymer composites from waste of major polluting industries and investigation on their physico-mechanical and wear properties," *Polymer Composites*, vol. 40, no. 3, pp. 1142–1157, 2019.

[61] S. N. Taqui, R. Yahya, A. Hassan, N. Nayak, and A. A. Syed, "Development of sustainable dye adsorption system using nutraceutical industrial fennel seed spent—studies using Congo red dye," *International Journal of Phytoremediation*, vol. 19, no. 7, pp. 686–694, 2017.

[62] S. J. Ukkund, P. Puthiyillam, A. E. Anqi et al., "A recent study on remediation of direct blue 15 dye using halloysite nanotubes," *Applied Sciences*, vol. 11, no. 17, p. 8196, 2021.

[63] S. J. Ukkund, P. Puthiyillam, H. M. Alshehri et al., "Adsorption method for the remediation of brilliant green dye using halloysite nanotube: isotherm, kinetic and modeling studies," *Applied Sciences*, vol. 11, no. 17, p. 8088, 2021.

[64] M. A. H. Dhaif-Allah, S. N. Taqui, U. T. Syed, and A. A. Syed, "Kinetic and isotherm modeling for acid blue 113 dye adsorption onto low-cost nutraceutical industrial fenugreek seed spent," *Applied Water Science*, vol. 10, no. 2, pp. 1–16, 2020.

[65] S. N. Taqui, U. T. Syed, R. T. Syed, M. S. Alqahtani, M. Abbas, and A. A. Syed, "Bioremediation of textile industrial effluents using nutraceutical industrial spent: laboratory-scale demonstration of circular economy," *Nanomaterials*, vol. 12, no. 10, p. 1684, 2022.

[66] T. Nharingo and M. Moyo, "Application of *Opuntia ficus-indica* in bioremediation of wastewaters. A critical review," *Journal of Environmental Management*, vol. 166, pp. 55–72, 2016.

[67] M. R. Haris and K. Sathasivam, "The removal of methyl red from aqueous solutions using banana pseudostem fibers," *American Journal of Applied Sciences*, vol. 6, no. 9, pp. 1690–1700, 2009.

[68] K. Pandey, G. Prasad, and V. Singh, "Copper(II) removal from aqueous solutions by fly ash," *Water Research*, vol. 19, no. 7, pp. 869–873, 1985.

[69] H. Yoshida, H. Nishihara, and T. Kataoka, "Adsorption of BSA on strongly basic chitosan: equilibria," *Biotechnology and Bioengineering*, vol. 43, no. 11, pp. 1087–1093, 1994.

[70] S. Wang, H. Li, S. Xie, S. Liu, and L. Xu, "Physical and chemical regeneration of zeolitic adsorbents for dye removal in wastewater treatment," *Chemosphere*, vol. 65, no. 1, pp. 82–87, 2006.

[71] I. Langmuir, "The constitution and fundamental properties of solids and liquids. Part I. Solids," *Journal of the American Chemical Society*, vol. 38, no. 11, pp. 2221–2295, 1916.

[72] T. W. Weber and R. K. Chakravorti, "Pore and solid diffusion models for fixed-bed adsorbers," *AICHE Journal*, vol. 20, no. 2, pp. 228–238, 1974.

[73] H. Freundlich, "Over the adsorption in solution," *The Journal of Physical Chemistry*, vol. 57, no. 385471, pp. 1100–1107, 1906.

[74] M. Tempkin and V. Pyzhev, "Kinetics of ammonia synthesis on promoted iron catalyst," *Acta Physico-Chimica USSR*, vol. 12, no. 1, p. 327, 1940.

[75] D. S. Jovanović, "Physical adsorption of gases," *Kolloid-Zeitschrift und Zeitschrift für Polymere*, vol. 235, no. 1, pp. 1203–1213, 1969.

[76] O. Redlich and D. L. Peterson, "*A useful adsorption isotherm*," *Journal of Physical Chemistry*, vol. 63, no. 6, pp. 1024–1024, 1959.

[77] R. Sips, "On the structure of a catalyst surface," *The Journal of Chemical Physics*, vol. 16, no. 5, pp. 490–495, 1948.

[78] C. Radke and J. Prausnitz, "Thermodynamics of multi-solute adsorption from dilute liquid solutions," *AICHE Journal*, vol. 18, no. 4, pp. 761–768, 1972.

[79] J. Toth, "State equation of the solid-gas interface layers," *Models in Chemistry*, vol. 69, pp. 311–328, 1971.

[80] W. R. Vieth and K. Sladek, "A model for diffusion in a glassy polymer," *Journal of Colloid Science*, vol. 20, no. 9, pp. 1014–1033, 1965.

[81] K. Iyer and A. Kunju, "Extension of Harkins-Jura adsorption isotherm to solute adsorption," *Colloids and Surfaces*, vol. 63, no. 3-4, pp. 235–240, 1992.

[82] S. K. Lagergren, "About the theory of so-called adsorption of soluble substances," *Sven. Vetenskapsakad. Handingarl*, vol. 24, pp. 1–39, 1898.

[83] Y.-S. Ho and G. McKay, "Sorption of dye from aqueous solution by peat," *Chemical Engineering Journal*, vol. 70, no. 2, pp. 115–124, 1998.

[84] E. C. Lopes, F. S. C. dos Anjos, E. F. S. Vieira, and A. R. Cestari, "An alternative Avrami equation to evaluate kinetic parameters of the interaction of Hg(II) with thin chitosan membranes," *Journal of Colloid and Interface Science*, vol. 263, no. 2, pp. 542–547, 2003.

[85] M. Alkan, Ö. Demirbaş, and M. Doğan, "Adsorption kinetics and thermodynamics of an anionic dye onto sepiolite," *Microporous and Mesoporous Materials*, vol. 101, no. 3, pp. 388–396, 2007.

[86] H.-L. Wang, J.-L. Chen, and Z.-C. Zhai, "Study on thermodynamics and kinetics of adsorption of p-toluidine from aqueous solution by hypercrosslinked polymeric adsorbents," *Environmental Chemistry-Beijing-*, vol. 23, no. 2, pp. 192–196, 2004.

[87] G. Boyd, A. Adamson, and L. Myers Jr., "The exchange adsorption of ions from aqueous solutions by organic zeolites. II. Kinetics[1]," *Journal of the American Chemical Society*, vol. 69, no. 11, pp. 2836–2848, 1947.